

# Sulforaphane Can Protect Lens Cells Against Oxidative Stress: Implications for Cataract Prevention

Hanruo Liu,<sup>1</sup> Andrew J. O. Smith,<sup>1</sup> Martin C. Lott,<sup>1,2</sup> Yongping Bao,<sup>3</sup> Richard P. Bowater,<sup>1</sup> John R. Reddan,<sup>4</sup> and Ian Michael Wormstone<sup>1</sup>

<sup>1</sup>School of Biological Sciences, University of East Anglia, Norwich, United Kingdom

<sup>2</sup>School of Computing Sciences, University of East Anglia, Norwich, United Kingdom

<sup>3</sup>Norwich Medical School, University of East Anglia, Norwich, United Kingdom

<sup>4</sup>Oakland University, Rochester, Michigan

Correspondence: Ian Michael Wormstone, School of Biological Sciences, University of East Anglia, Norwich Research Park, Norwich, UK NR4 7TJ; i.m.wormstone@uea.ac.uk.

Submitted: January 15, 2013

Accepted: June 16, 2013

Citation: Liu H, Smith AJO, Lott MC, et al. Sulforaphane can protect lens cells against oxidative stress: implications for cataract prevention. *Invest Ophthalmol Vis Sci.* 2013;54:5236-5248. DOI:10.1167/iovs.13-11664

**PURPOSE.** Protecting the lens against oxidative stress is of great importance in delaying the onset of cataract. Isothiocyanates, such as sulforaphane (SFN), are proposed to provide cytoprotection against oxidative stress. We therefore tested the ability of SFN to perform this role in lens cells and establish its ability to delay the onset of cataract.

**METHODS.** The human lens epithelial cell line FHL124 and whole porcine lens culture systems were used. The ApoTox-Glo Triplex Assay was used to assess FHL124 cell survival, cytotoxicity, and apoptosis. The MTS assay was used to assess cell populations. To determine levels of DNA strand breaks, the alkaline comet assay was performed and quantified. Lactate dehydrogenase levels in the medium were evaluated to reflect cell damage/death. To assess level of gene expression, an Illumina whole-genome HT-12 v4 beadchip was used. Protein expression was determined by Western blot and immunocytochemistry.

**RESULTS.** Exposures of 30  $\mu\text{M}$   $\text{H}_2\text{O}_2$  to FHL124 cells caused a reduction in cell viability and increased cytotoxicity/apoptosis; these effects were significantly inhibited by 24-hour pretreatment with 1  $\mu\text{M}$  SFN. In addition, 1  $\mu\text{M}$  SFN significantly reduced  $\text{H}_2\text{O}_2$ -induced DNA strand breaks. When applied to cultured porcine lenses, SFN protected against  $\text{H}_2\text{O}_2$ -induced opacification. Illumina whole-genome HT-12 v4 beadchip microarray data revealed eight genes upregulated following 24-hour exposure to 1- and 2- $\mu\text{M}$  SFN, which included NQO1 and TXNRD1. This pattern was confirmed at the protein level. Nrf2 translocated to the nucleus in response to 0.5- to 2.0- $\mu\text{M}$  SFN exposure

**CONCLUSIONS.** The dietary component SFN demonstrates an ability to protect human lens cells against oxidative stress and thus could potentially delay the onset of cataract.

**Keywords:** sulforaphane, Isothiocyanates, antioxidant, diet, lens, cataract

Cataract renders millions in the world blind and is notably a disease that largely afflicts the elderly.<sup>1</sup> In the world, management of cataract is a significant strain on health care budgets.<sup>2</sup> At present, the only means to treat cataract is by surgical intervention<sup>3</sup> and it is predicted that 32 million operations will be performed annually by 2020. Delaying the onset of cataract is therefore a major health care priority across the globe.

Free radical production leading to oxidative stress is an initiating factor in the development of maturity-onset cataract.<sup>4</sup> Free radicals are atomic or molecular species with at least one unpaired electron in the outermost shell and any free radical involving oxygen can be referred to as reactive oxygen species (ROS). Unpaired electrons cause the free radicals to be highly reactive and likely to take part in chemical reactions.<sup>5</sup> ROS molecules include superoxide anion ( $\text{O}_2^{\bullet-}$ ), hydroxyl radical ( $\bullet\text{OH}$ ), and hydrogen peroxide ( $\text{H}_2\text{O}_2$ ). Contrary to  $\text{O}_2^{\bullet-}$  and  $\bullet\text{OH}$ , which are extremely unstable and react at or near their site of formation,  $\text{H}_2\text{O}_2$  is less reactive, freely diffusible, and relatively long-lived.<sup>5</sup> ROS can be generated either endogenously or exogenously in relation to human cells. Endogenous sources include mito-

chondria, peroxisomes, lipoxygenases, nicotinamide adenine dinucleotide phosphate (NADPH) oxidase, and cytochrome P450.<sup>5</sup> Exogenous sources include UV light, ionizing radiation, chemotherapeutics, inflammatory cytokines, and environmental toxins.<sup>6,7</sup> It is widely believed that a rise in the intracellular levels of ROS will damage various cell components, interrupt physiological functions, and lead to aging and various oxidative stress-associated disorders.<sup>7</sup> The damage can consist of protein modification, lipid peroxidation, DNA base damage, and fragmentation, all of which have been proposed to contribute to cataractogenesis. The lens, like other organs, has a well-designed defense system and uses primary defenses against ROS to repair, recover, or degrade damaged molecules.<sup>8</sup> The lens is able to defend itself against oxidation using antioxidants from either enzymatic or nonenzymatic systems.<sup>4,9</sup> Primary antioxidants include nonenzymatic (e.g., glutathione, vitamin C, vitamin E, and carotenoids) and enzymatic (e.g., superoxide dismutase, glutathione peroxidase, and catalase) systems. The lens is known to contain antioxidant defense systems. One example of a lens antioxidant defense system is the glutathione-dependent thioltransferase,<sup>10-12</sup> which may be critical in maintaining the lens in a

reduced state by cleaving protein-thiol mixed disulfide bonds formed upon the oxidation of lens proteins. Another example is the NADPH-dependent thioredoxin/thioredoxin reductase system,<sup>13</sup> which is very effective in reducing protein-protein disulfide bonds and maintaining thiol/disulfide homeostasis.<sup>8,14</sup> Under oxidative stress, some of these defense systems can be upregulated.<sup>15,16</sup> A healthy lens uses its various antioxidants and oxidation defense enzymes to maintain crystallins, the structural proteins of the lens, in a reduced state. This is necessary to maintain lens transparency<sup>17</sup>; however, in the aging lens, protection and repair mechanisms against oxidative stress slowly deteriorate or become ineffective and so the lens is less able to counteract the effects of H<sub>2</sub>O<sub>2</sub> or other oxidants; thus, transparency is lost and cataract can occur.<sup>18</sup> Therefore, enhancing the antioxidant defense systems within the lens is a worthwhile aim and dietary supplements provide a logical means to achieve this.

Isothiocyanates (ITCs), which are derived from glucosinolates found in cruciferous vegetables, are characterized by sulfur-containing N = C = S functional groups. These include allyl ITC from cabbage, mustard, and horseradish; benzyl isothiocyanate; phenethyl ITC from watercress and garden cress; and sulforaphane (SFN) from broccoli, cauliflower, brassicas, and kale.<sup>19</sup> ITCs can inhibit many types of tumor formation in animal models and their consumption is inversely correlated with the risk of cancer in humans.<sup>20</sup> Protective mechanisms of ITCs have been proposed. Such mechanisms include the induction of phase II detoxification enzymes and inhibition of phase I carcinogen-activating enzymes.

SFN is a product of hydrolytic conversion of 4-methylsulphinylbutyl glucosinolate (glucoraphanin) by an endogenous myrosinase.<sup>21</sup> It has been identified as a very potent chemopreventive agent in numerous animal carcinogenesis models as well as cell culture models, exerting its chemopreventive effects through regulation of diverse molecular mechanisms.<sup>22</sup> The most studied role of SFN in chemoprevention is its ability to induce phase II detoxification enzymes as well as cell cycle arrest and apoptosis. Experimental evidence suggests that SFN activates NF-E2 p45-related factor-2 transcription factor (Nrf2) in binding antioxidant response elements in the promoter regions of target genes, thereby increasing cellular defenses against oxidative stress.<sup>22,23</sup> It is reported that most broccoli cultivars contain 2 to 10 μmol/g glucosinolates.<sup>20</sup> If cooked, almost 100% of the glucosinolate is converted to SFN. Intake of 200 μmol broccoli ITCs (mainly SFN) in humans has been reported to result in SFN plasma levels in the low micromolar range.<sup>24</sup> Therefore, the aim of this current research was to assess the ability of SFN to protect human lens epithelial cells against oxidative stress and lens opacification.

## METHODS

All reagents were purchased from Sigma (Poole, Dorset, UK) unless otherwise stated.

### Cell Culture

FHL124 is a nonvirally transformed cell line generated from human capsule-epithelial explants,<sup>25</sup> showing a 99.5% homology (in transcript profile) with the native lens epithelium.<sup>26</sup> FHL124 cells were routinely cultured at 35°C in a humidified atmosphere of 95% air and 5% CO<sub>2</sub>, in Eagle's Minimum Essential Medium (EMEM) supplemented with 5% vol/vol fetal calf serum (Gibco, Paisley, UK) and 50 μg/mL gentamicin. FHL124 cells were seeded on 35-mm tissue-culture dishes

(30,000/dish for Western blot, 30,000/dish for microarrays, 10,000/coverslip for immunocytochemistry, 35,000/dish for alkaline comet assay), and 96-well plates (5000/well for ApoTox-Glo Triplex Assay (Promega, Madison, WI), 10,000/dish for lactate dehydrogenase [LDH] Assay).

### ApoTox-Glo Triplex Assay

FHL124 cells were seeded on 96-well plates at a density of 5000 cells per well. Twenty-four hours before addition of experimental conditions, culture medium was replaced with 200 μL serum-free EMEM. The medium was then removed from each well and replaced with fresh EMEM and test compounds where appropriate. Plates were incubated at 35°C, 5% CO<sub>2</sub> for the experimental duration (up to 72 hours). The ApoTox-Glo Triplex Assay (Promega) was used to measure FHL124 cell viability, cytotoxicity, and apoptosis following manufacturer's instructions. Briefly, viability and cytotoxicity are measured by fluorescent signals produced when either live-cell or dead-cell proteases cleave added substrates GF-AFC (viability) and bis-AAF-R110 (cytotoxicity). Fluorescence of the cleaved products is proportional to either viability or cytotoxicity. GF-AFC can enter cells and is therefore only cleavable by live-cell protease, which incidentally becomes inactive when cell membrane activity is lost; bis-AAF-R110 cannot enter the cell, and is cleaved only by dead-cell protease leaked from cells lacking membrane integrity. Both cleaved substrates have different excitation and emission spectra. Apoptosis is measured by the addition of a luminogenic caspase-3/7 substrate (Caspase-Glo 3/7, a component of the ApoTox-Glo Triplex Assay; Promega), which is cleaved in apoptotic cells to produce a luminescent signal. Fluorescence was measured at 380<sub>Ex</sub>/510<sub>Em</sub> (viability), 485<sub>Ex</sub>/520<sub>Em</sub> (cytotoxicity), and luminescence (apoptosis) with a FLUOstar Omega plate reader (BMG LabTech, Aylesbury, Bucks, UK).

### MTS Assay

A cell proliferation assay (CellTiter 96 Aqueous; Promega) was used in accordance with the manufacturer's instructions to assess the viability of the cells. This assay is a colorimetric method for determining the number of viable cells in proliferation. The assay is based on the cellular conversion of a tetrazolium salt (MTS) into a formazan product. The resultant absorbance is directly proportional to the number of living cells in culture. In brief, 5000 cells were seeded in 96-well plates for 24 hours before the medium was replaced with 200 μL serum-free EMEM and incubated for a further 24 hours. The medium was then removed from each well and replaced with 200 μL fresh EMEM; test compounds were added where appropriate. Cells were maintained in experimental conditions for 24 or 48 hours. Then, 25 μL CellTiter 96 Aqueous One Solution was added directly to the culture wells and incubated for the final hour. Absorbance was measured at 490 nm with a spectrophotometric plate reader (FLUOstar Omega plate reader; BMG LabTech). Cell viability was expressed as a percentage, with 100% representing the signal from untreated cells and 0% representing the background signal from empty wells.

### Cell Death Assay (LDH Assay)

A nonradioactive cytotoxicity assay (Cyto Tox 96R; Roche, Welwyn Garden City, UK) was used to measure the release of LDH from the cultured human lens cells and porcine whole lens cultures. The procedure followed the manufacturer's protocol. The plate was read at 490 nm with a FLUOstar Omega plate reader (BMG LabTech).

## Alkaline Comet Assay

The alkaline comet assay, also called single-cell gel electrophoresis, is a sensitive and rapid technique for quantifying and analyzing DNA strand breaks in individual cells. FHL124 cells were seeded onto 35-mm plastic culture dishes at a density of 35,000 cells per dish and grown until approximately 70% confluent. At this time point, the medium was removed from each dish and replaced with 1.5 mL serum-free EMEM for 24 hours before placing the cells in experimental conditions for a further 24 hours. Cells were pretreated with 1  $\mu$ M SFN for 24 hours before exposure to 30  $\mu$ M H<sub>2</sub>O<sub>2</sub> and cells incubated at 35°C, 5% CO<sub>2</sub>. The cells were washed with ice-cold PBS, harvested, counted, resuspended in PBS containing 10% dimethyl sulfoxide and frozen at -80°C until the alkaline comet assay was performed. Samples were defrosted and approximately 25,000 cells per sample were centrifuged at 108g for 5 minutes at 4°C. Pellets were resuspended in 0.6% low melting point agarose, dispensed in duplicate onto glass microscope slides (precoated in 1% normal melting point agarose), and allowed to set on ice, under a glass coverslip. Once set, the coverslips were removed and slides transferred into ice-cold lysis buffer (100 mM disodium EDTA [Fisher Scientific, Loughborough, UK], 2.5 M NaCl [Fisher Scientific], 10 mM Tris-HCl [Formedium; Fisher Scientific], pH 10.0 with 1% Triton X-100 added immediately before use) for 1 hour. Slides were washed twice with ice-cold dH<sub>2</sub>O for 10 minutes, transferred to a flatbed electrophoresis tank, and incubated in freshly prepared ice-cold electrophoresis buffer (300 mM NaOH [BDH Merck Ltd., Poole, Dorset, UK], 1 mM disodium EDTA, pH 13) for 30 minutes, followed by electrophoresis in the same buffer at 21 V (1 V/cm) for 30 minutes. Procedures were performed protected from direct light. Slides were drained of electrophoresis buffer and flooded with neutralization buffer (0.4 M Tris-HCl, pH 7.5) for 30 minutes, washed twice in dH<sub>2</sub>O for 10 minutes, and dried at 37°C. Slides were stained with SYBR Green I nucleic acid stain diluted from a 10,000 X stock in 1X TE buffer (10 mM Tris-HCl, 1 mM EDTA) for 5 minutes protected from light at room temperature, drained, and dried at room temperature before visualization. For each sample, 100 comets were randomly analyzed (50 per gel), with images captured by fluorescence microscopy (Axioplan 2; Zeiss, Cambridge, UK) and comets scored using Comet Assay IV Lite analysis software (Perceptive Instruments, Bury St Edmunds, UK).

## Microarray Analysis

FHL124 cells were seeded onto 35-mm plastic culture dishes at a density of 35,000 cells per dish and grown until approximately 70% confluent. At this time point, the medium was removed from each dish and replaced with 1.5 mL serum-free EMEM for 24 hours before placing the cells in experimental conditions for a further 24 hours. One dish was used per experimental condition; the experiment was carried out on four separate occasions. A microarray platform was selected to provide a comprehensive view of the gene activity under the different conditions. To achieve this, the commercially available Human-HT12.v4 Expression Bead Chip (BD-25-113; Illumina, San Diego, CA) array platform was used. RNA was extracted from FHL124 cells using an RNeasy mini kit (Qiagen Ltd., Crawley, UK). The monolayer of cells was lysed by adding 350  $\mu$ L buffer RLT containing 2- $\beta$ -mercaptoethanol, to each culture dish. The cell lysate was collected using a cell scraper. The cell lysate was then transferred into a sterile microcentrifuge tube and was passed through a 20-gauge needle (0.9-nm diameter), fitted to an RNase-free syringe, three times. This process homogenizes the cells allowing the RNA to be released from all FHL124 cells; 350  $\mu$ L 70% ethanol was added to the homogenized lysate, and was

mixed via pipetting. The ethanol was added to the lysate to create conditions that promote selective binding of RNA to the RNeasy silica-gel membrane. Then, 700  $\mu$ L of the solution was transferred to an RNeasy mini column placed in a 2-mL collection tube. The columns were centrifuged for 30 seconds at 6000g and the flow-through discarded. A series of washes using different buffers was carried out to produce the pure RNA. Then, 700  $\mu$ L RW1 buffer was added to the RNeasy mini column, centrifuged for 30 seconds, and removal of flow-through was carried out. The RNeasy mini column was fitted to one new collection tube and washed two times with 500  $\mu$ L RPE buffer with an initial centrifugation for 15 seconds and the second centrifugation for 2 minutes to dry the RNeasy silica-gel membrane containing the RNA. Using 50  $\mu$ L RNeasy free water, the RNA was eluted from the column into a sterile 1.5-mL microcentrifuge tube and centrifuged for 1 minute. RNA samples were shipped on dry ice to a commercial microarray facility. RNA quantity and quality was assessed using the NanoDrop ND-1000 spectrophotometer (NanoDrop Technologies, Wilmington, DE) and an Agilent RNA pico labchip (Wokingham, UK); only samples with an RNA integrity number greater than or equal to 9 were used in the study. Average RNA yields per dish were 879  $\pm$  248 ng, 1003  $\pm$  231 ng, and 975  $\pm$  211 ng for the 0-, 1-, and 2- $\mu$ M SFN-treated groups respectively. From all samples, 100 ng RNA was processed according to the Illumina Whole-Genome Gene Expression Direct Hybridisation Assay Guide, using the Ambion Kit: Illumina TotalPrep-96 RNA Amplification Kit. Qualitative and quantitative quality control was performed on the labeled cRNA and 1.5  $\mu$ g labeled cRNA was hybridized to a HumanHT-12.v4 Beadchip and scanned by the Illumina BeadArray reader.

Illumina microarray (BeadArray) unnormalized probe profile data were analyzed using the Bioconductor package (provided in the public domain at <http://www.bioconductor.org>) in R (provided in the public domain at <http://www.r-project.org>). First, the data from different chips were loaded into R to be background corrected, quantile normalized, and variance stabilized.<sup>27</sup> The normalized data from all the arrays have been deposited in the Array Express database with an accession number (E-MEXP-3923). Lists of differentially expressed genes were computed by using the eBAYES statistic<sup>28</sup> to compute a *P* value. Additionally, the fold change (FC) of each gene was computed, that is, the ratio of average expression level between the two groups. Differentially expressed genes were determined by using a combination of FC and adjusted *P* value (*q* value) threshold criteria, as that has been found to discover genes more likely to play a physiological role.<sup>29</sup> The Benjamini and Hochberg method<sup>30</sup> is used to compute *q* values and control the false discovery rate, that is, the proportion of genes identified as being significant but that later transpire as being false leads. Genes were identified as being significant if FC was greater than or equal to 1.3 and *q* value was greater than or equal to 0.20.

## Western Blot Analysis

Cell lysates from FHL124 cells were prepared using Daub's lysis buffer supplemented with 1 mM phenylmethylsulfonyl fluoride (PMSF) and 10  $\mu$ g/mL aprotinin for 20 minutes on ice and centrifuged at 16,060g for 10 minutes. The protein content was determined by the BCA assay (Bio-Rad, Hemel Hempstead, UK) so that equal amounts of protein per sample were loaded onto 8% SDS-polyacrylamide gels and transferred to PVDF membrane using a semidry transfer cell. The membrane was blocked with PBS containing 5% wt/vol nonfat dry milk and 0.1% vol/vol Tween-20, hybridized with primary antibody followed by incubation with secondary antibody (Amersham Biosciences, Bucks, UK). Proteins were detected using the ECL plus blotting analysis system (Amersham Biosciences).

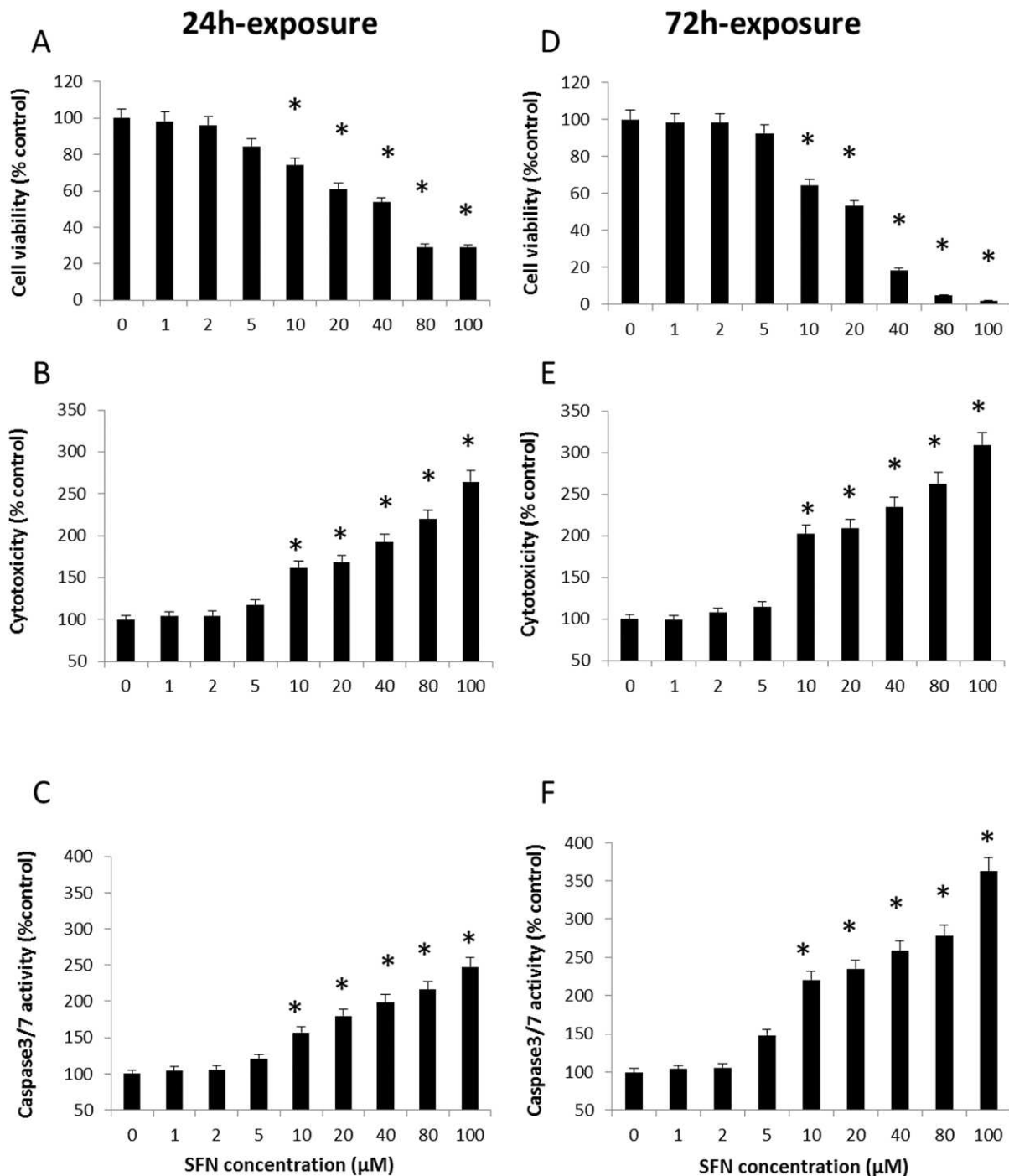


**FIGURE 1.** Concentration-dependent effects of SFN on FHL124 cell viability (A, D), cytotoxicity (B, E), and apoptosis (C, F) detected by the ApoTox-Glo Triplex Assay following a 24- (A–C) and 72-hour (D–F) culture period with SFN. The data are presented as mean  $\pm$  SEM ( $n = 4$ ). The asterisk indicates a significant difference between the treated group and untreated controls ( $P \leq 0.05$ ; ANOVA with Dunnett's post hoc test).

### Immunocytochemistry

FHL124 cells were grown on sterile glass coverslips contained within a 35-mm plastic culture dish at a density of 10,000 cells per coverslip and treated with 0-, 0.5-, 1-, and 2- $\mu\text{M}$  SFN for 24 hours. Cells were fixed with 4% formaldehyde in PBS for 30 minutes and permeabilized with PBS containing 0.5% Triton X-100 for 30 minutes. Three washes were made in PBS-BSA-Igepal (0.02% wt/vol and 0.05% vol/vol, respectively). Nonspecific sites were blocked with normal goat or donkey serum (1:50 in 1% wt/

vol BSA in PBS). NQO1 antibody and TXNRD1 antibody were diluted 1:200 and Nrf2 antibody was diluted 1:100 in 1% BSA in PBS and applied overnight at 4°C followed by washing three times for 5 minutes with shaking with 0.02% BSA, 0.05% IGEPAL in PBS. NQO1 and TXNRD1 were visualized using ALEXA 488-conjugated goat anti-mouse secondary antibody and nrf2 using ALEXA 488-conjugated donkey anti-rabbit secondary antibody diluted 1:100 in 1% BSA in PBS (Molecular Probes, Leiden, The Netherlands). Chromatin was stained with 4',6-Diamidino-2-Phenylindole, Dihydrochloride (DAPI) to reveal nuclei (1:100 in

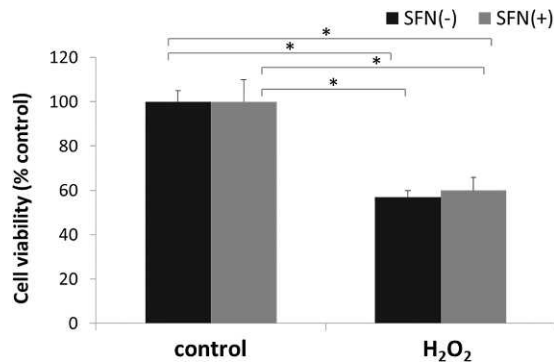


**FIGURE 2.** The viability of FHL124 cells exposed to 30  $\mu\text{M}$   $\text{H}_2\text{O}_2$  together with 1  $\mu\text{M}$  SFN over a 24-hour culture period using the MTS assay. The data are expressed as % cell survival in comparison with control, represented as 100%. Each *column* represents the mean  $\pm$  SEM of four independent experiments. The *asterisk* represents a significant difference between the indicated groups ( $P \leq 0.05$ ; ANOVA with Tukey's post hoc test).

1% wt/vol BSA in PBS) (Molecular Probes). The stained preparations were again washed extensively and mounted on microscope slides with Hydromount mounting medium (National Diagnostics, Hull, UK). Images were viewed using fluorescence microscopy (Axioplan 2; Zeiss), and applicable images were quantified using ImageJ1.45s analysis software (available in the public domain at <http://rsbweb.nih.gov/ij/>).<sup>31</sup>

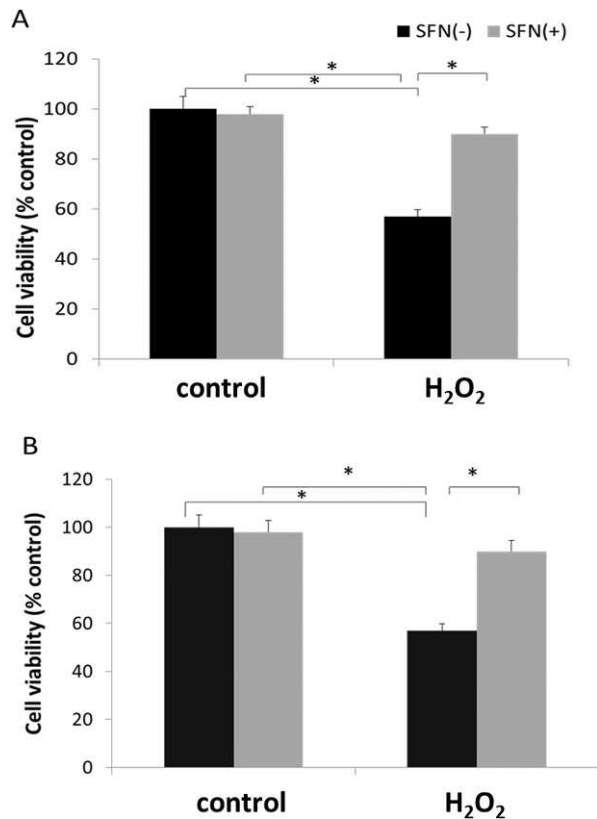


**FIGURE 3.** The viability of FHL124 cells exposed to 1  $\mu\text{M}$  SFN for 24 hours, followed by 30  $\mu\text{M}$   $\text{H}_2\text{O}_2$  in the absence of SFN (A) and in the presence of SFN (B) for a further 24 hours using the MTS assay. The data are expressed as % cell survival in comparison with control, represented as 100%. Each *column* represents the mean  $\pm$  SEM of four independent experiments. The *asterisk* represents a significant difference between indicated groups ( $P \leq 0.05$ ; ANOVA with Tukey's post hoc test).

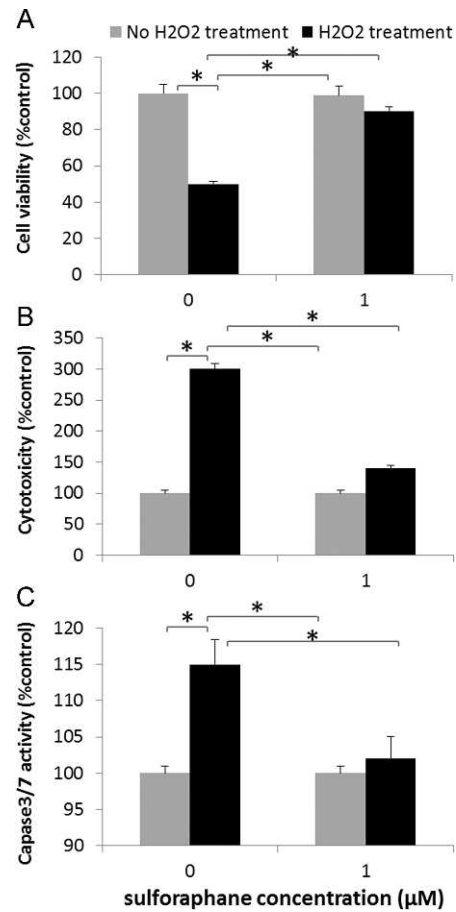


**FIGURE 4.** SFN protection against oxidative stress induced loss of cell viability (A), cytotoxicity (B), and apoptosis (C), following a 24-hour experimental period, determined using the ApoTox-Glo Assay. Cells were pretreated with 1  $\mu\text{M}$  SFN for 24 hours before exposure to 30  $\mu\text{M}$   $\text{H}_2\text{O}_2$ . Data are presented as mean  $\pm$  SEM ( $n = 4$ ). The *asterisk* indicates a significant difference between the indicated groups ( $P \leq 0.05$ ; ANOVA with Tukey's post hoc test).

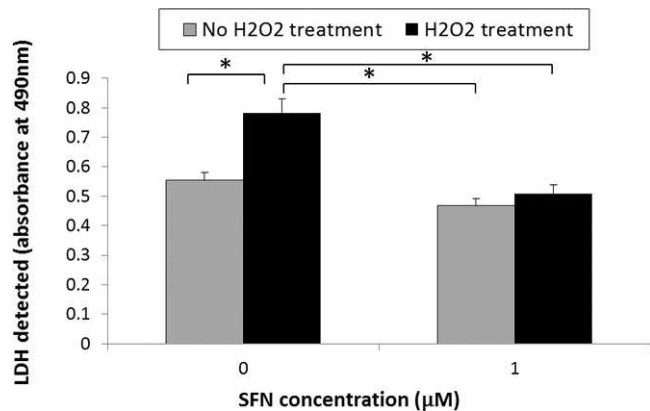


**FIGURE 5.** SFN protection against oxidative stress-induced cell damage/death, following a 24-hour experimental period, determined using the LDH assay. Cells were pretreated with 1  $\mu\text{M}$  SFN for 24 hours before exposure to 30  $\mu\text{M}$   $\text{H}_2\text{O}_2$ . Data are expressed as mean  $\pm$  SEM ( $n = 4$ ). The *asterisk* represents a significant difference between the indicated groups ( $P \leq 0.05$ ; ANOVA with Tukey's post hoc test).

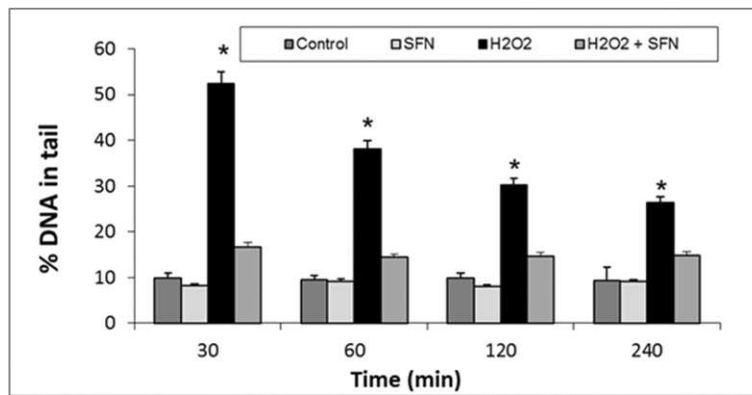


**FIGURE 6.** SFN suppression of DNA damage of FHL124 cells induced by oxidative stress detected using the comet assay following a 30-, 60-, 120-, or 240-minute experimental period. Cells were pretreated with 1  $\mu$ M SFN for 24 hours before exposure to 30  $\mu$ M H<sub>2</sub>O<sub>2</sub>. DNA strand breaks were measured by the alkaline comet assay and tails were measured for at least 100 comets per sample. Data are presented as mean  $\pm$  SEM pooled from four individual experiments. The *asterisk* represents a significant difference between the indicated groups ( $P \leq 0.05$ ; ANOVA with Tukey's post hoc test).

### Whole Pig Lens Culture

Fresh porcine eyes were obtained from a local slaughterhouse (Felthorpe, Norfolk, UK). The tissue collection conformed to the ARVO Statement for the Use of Animals in Ophthalmic and Vision Research. Eyes were placed in sterile containers and

covered with Eagle's minimum essential medium (EMEM) containing 200 U/mL penicillin and 200  $\mu$ g/mL streptomycin. They were stored at 4°C before dissection. Within 24 hours postmortem, lenses were dissected by anterior approach following cornea removal and incubated in 3 mL bicarbonate-

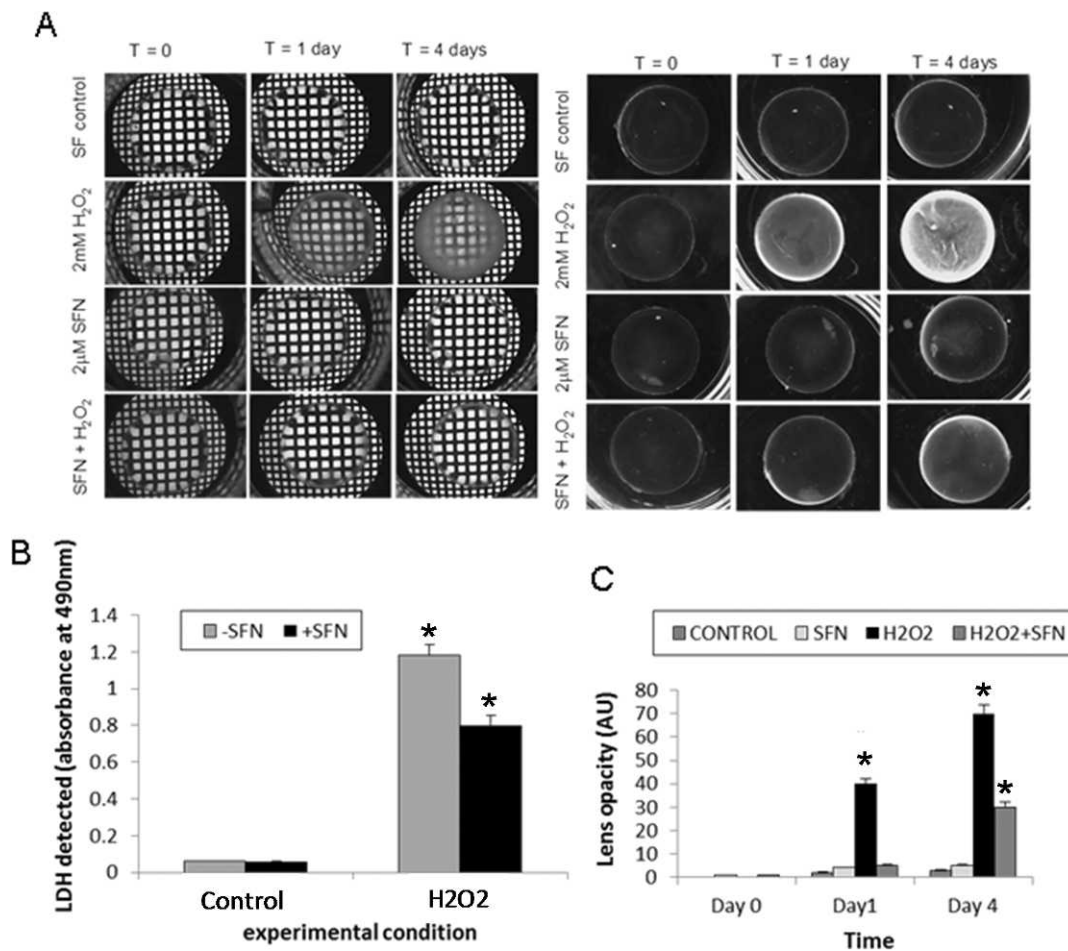


**FIGURE 7.** SFN reduces hydrogen peroxide-induced lens opacity. (A) Representative bright-field and dark-field images of whole pig lens organ cultures over time. (B) Pooled data showing LDH levels within the culture medium at end point; data are presented as mean  $\pm$  SEM ( $n = 4$ ). (C) Quantification of lens opacity over time ( $n = 4$ ); data are presented as mean  $\pm$  SEM ( $n = 4$ ). SFN was applied at 2  $\mu$ M and H<sub>2</sub>O<sub>2</sub> at 2 mM. The *asterisk* represents a significant difference from all other groups ( $P \leq 0.05$ ; ANOVA with Tukey's post hoc test).

TABLE 1. SFN (1  $\mu$ M) Induced Gene Expression Increase Detected in FHL124 Epithelial Cells Using Illumina Gene Microarray

Official Symbol	Official Full Name	Location	Summary	FC	P Value	q Value
<i>NQO1</i>	NAD(P)H dehydrogenase, quinone 1	16q22.1	This protein's enzymatic activity prevents the 1-electron reduction of quinones that results in the production of radical species	2.04735	1.51E-05	0.087413526
<i>OKL38</i>	Oxidative stress-induced growth inhibitor	16q23.3	Encodes an oxidative stress response protein that regulates cell death	1.96899	3.04E-07	0.010537
<i>LOC392437</i>	Unknown	Unknown	Unknown	1.63879	0.000023	0.113791741
<i>TXNRD1</i>	Thioredoxin reductase 1	12q23-q24.1	This gene encodes a member of the family of pyridine nucleotide oxidoreductases and plays a role in selenium metabolism and protection against oxidative stress	1.60769	1.41E-05	0.087413526
<i>PIR</i>	pirin (iron-binding nuclear protein)	XP22.2	The encoded protein is an Fe(II)-containing nuclear protein expressed in all tissues It can act as a transcriptional cofactor and is involved in the regulation of DNA transcription and replication	1.41567	4.59E-06	0.053056757
<i>G6PD</i>	Glucose-6-phosphate dehydrogenase	xq28	This gene encodes glucose-6-phosphate dehydrogenase whose main function is to produce NADPH	1.39306	2.8E-06	0.048589621
<i>EPHX1</i>	Epoxide hydrolase 1, microsomal (xenobiotic)	1q42.1	Epoxide hydrolase is a critical biotransformation enzyme, which functions in both the activation and detoxification of epoxides	1.37074	1.17E-05	0.087413526
<i>FTL</i>	Ferritin, light polypeptide	19q13.33	FTL encodes the light subunit of the ferritin protein It affects the rates of iron uptake and release in different tissues	1.35383	5.39E-05	0.169818382
<i>PANX2</i>	Pannexin 2	22Q13.33	This protein and pannexin 1 are abundantly expressed in the central nervous system and are coexpressed in various neuronal populations	1.32656	2.69E-05	0.116426773

All genes presented were increased  $\geq 1.3$ -fold in the SFN-treated group relative to nontreated control and were statistically different ( $q \leq 0.20$ ; eBAYES *t*-test with Benjamini-Hochberg correction).

CO<sub>2</sub>-buffered EMEM (pH 7.4), containing 100 U/mL penicillin, 100  $\mu$ g/mL streptomycin, 0.25  $\mu$ g/mL amphotericin, and 50  $\mu$ g/mL gentamicin at 35°C. After a preculture period of 24 to 72 hours to ensure no damage had arisen from the isolation procedure, lenses were exposed to 3 mL EMEM or 3 mL EMEM supplemented with SFN (2  $\mu$ M) for 24 hours before addition of H<sub>2</sub>O<sub>2</sub> (2 mM final concentration) or vehicle control. During the experimental period, lens images were taken at the starting point ( $t = 0$ ), 24-hour time point, and 4-day point using a charge-coupled device (CCD) camera (UVP, Cambridge, UK) with Synoptics software (GeneSnap; Synoptics, Cambridge, UK). At the end of 24 hours of culture in the presence of experimental conditions, the medium was collected to assay for LDH. Dark-field images of lenses taken using the CCD camera were measured for grayscale values with ImageJ1.45s analysis software (available in the public domain at <http://rsbweb.nih.gov/ij/>). Images captured at the start of the experimental period ( $t = 0$  days) were treated as background level for each lens. Subsequent grayscale values of images for each lens, captured at day 1 and day 4, were background corrected.

### Statistical Analyses

A *t*-test analysis was performed using Excel software (Microsoft, Redmond, WA) to determine any statistical difference between the two groups. One-way ANOVA with Tukey's post hoc analysis was used to assess multiple groups when all or many pairwise comparisons were of interest. One-way ANOVA with Dunnett's post hoc analysis was used to assess all groups

compared against one control group. A 95% confidence interval was used to assess significance.

## RESULTS

### Sulforaphane Effects on Cell Viability, Cytotoxicity, and Apoptotic Cell Death

Cell viability relative to the untreated control group was not significantly affected by SFN exposure of 5  $\mu$ M and below following 24- and 72-hour exposure periods (Figs. 1A, 1D). However, at SFN concentrations of 10  $\mu$ M and above, a significant reduction in cell viability was observed; this effect became more pronounced with increasing concentrations of SFN (Figs. 1A, 1D). A significant increase in cytotoxicity was also seen with SFN exposure between 20 and 100  $\mu$ M (Figs. 1B, 1E). Apoptosis was detected in the ApoTox-Glo Triplex Assay (Promega) using Caspase-Glo to detect Caspase 3/7 activity and, consistent with the other measurements, a significant increase was identified following 10- to 100- $\mu$ M SFN exposure (Figs. 1C, 1F).

### Sulforaphane Protection of Lens Cells Against Oxidative Stress

SFN concentrations of 5  $\mu$ M and less did not reduce viability of FHL124 cells and, thus, these concentrations could be used to assess putative protection of lens cells against oxidative insult (by hydrogen peroxide).

TABLE 2. SFN (2  $\mu$ M) Induced Gene Expression Increase Detected in FHL124 Epithelial Cells Using Illumina Gene Microarray

Official Symbol	Official Full Name	Location	Summary	FC	P Value	q Value
<i>OKL38</i>	Oxidative stress-induced growth inhibitor	16q23.3	Encodes an oxidative stress response protein that regulates cell death	2.18195	5.51E-08	0.001911616
<i>NQO1</i>	NAD(P)H dehydrogenase, quinone 1	16q22.1	This protein's enzymatic activity prevents the 1-electron reduction of quinones that results in the production of radical species	2.09728	1.06E-05	0.046724545
<i>LOC392437</i>	Unknown	Unknown	Unknown	1.74835	6.19E-06	0.046724545
<i>TXNRD1</i>	Thioredoxin reductase 1	12q23-q24.1	This gene encodes a member of the family of pyridine nucleotide oxidoreductases and plays a role in selenium metabolism and protection against oxidative stress	1.72358	3.18E-06	0.036786402
<i>PIR</i>	Pirin (iron-binding nuclear protein)	XP22.2	The encoded protein is an Fe(II)-containing nuclear protein expressed in all tissues It can act as a transcriptional cofactor and is involved in the regulation of DNA transcription and replication	1.56149	2.63E-07	0.004559489
<i>GCLM</i>	Glutamate-cysteine ligase, modifier subunit	1p22.1	Glutamate-cysteine ligase is the first rate limiting enzyme of glutathione synthesis	1.53588	5.97E-05	0.159341311
<i>FTL</i>	Ferritin, light polypeptide	19q13.33	FTL encodes the light subunit of the ferritin protein It affects the rates of iron uptake and release in different tissues	1.42567	1.06E-05	0.046724545
<i>EPHX1</i>	Epoxide hydrolase 1, microsomal (xenobiotic)	1q42.1	Epoxide hydrolase is a critical biotransformation enzyme, which functions in both the activation and detoxification of epoxides	1.37391	1.08E-05	0.046724545
<i>G6PD</i>	Glucose-6-phosphate dehydrogenase	xq28	This gene encodes glucose-6-phosphate dehydrogenase. Its main function is to produce NADPH	1.34738	0.000009	0.046724545

All genes presented were increased  $\geq 1.3$ -fold in the SFN-treated group relative to nontreated control and were statistically different ( $q \leq 0.20$ ; eBAYES *t*-test with Benjamini-Hochberg correction).

FHL124 cells were cotreated with 1  $\mu$ M SFN and 30  $\mu$ M H<sub>2</sub>O<sub>2</sub> for 24 hours and cell viability tested by the MTS assay (Fig. 2). The 30  $\mu$ M H<sub>2</sub>O<sub>2</sub> reduced FHL124 cell viability to 55% of the control population; 1  $\mu$ M SFN alone had no effect on cell viability, which did not significantly differ from the control group (Fig. 2). Cells cotreated with 1  $\mu$ M SFN and 30  $\mu$ M H<sub>2</sub>O<sub>2</sub> exhibited a reduction in the viable cell population, which was significantly different from the control group, but did not significantly differ from the cells treated with 30  $\mu$ M H<sub>2</sub>O<sub>2</sub> alone (Fig. 2), indicating no significant protection of the cells by SFN against H<sub>2</sub>O<sub>2</sub> toxicity using this approach.

To investigate whether SFN has indirect antioxidant properties that could elicit protection to lens cells against oxidative stress, FHL124 cells were incubated with 1  $\mu$ M SFN for 24 hours before exposure to 30  $\mu$ M H<sub>2</sub>O<sub>2</sub>. SFN was then removed (Fig. 3A) or retained (Fig. 3B) before adding H<sub>2</sub>O<sub>2</sub>. Figure 3B shows that addition of 30  $\mu$ M H<sub>2</sub>O<sub>2</sub> significantly reduced the viable cell population (again detected using the MTS assay), within 24 hours, such that levels were 56%  $\pm$  4% compared with the untreated control. FHL124 cells pretreated with 1  $\mu$ M SFN, before addition of 30  $\mu$ M H<sub>2</sub>O<sub>2</sub> and retained for the experimental duration, demonstrated a significant increase in the viable population relative to H<sub>2</sub>O<sub>2</sub> alone that was comparable with control populations. When FHL124 cells were incubated with SFN for 24 hours before its removal and subsequent H<sub>2</sub>O<sub>2</sub> addition, marked cytoprotection was still observed (Fig. 3A).

Due to the results of the MTS assay, the ApoTox-Glo Triplex Assay (Promega) was used so as to have an independent means of verifying the results. Exposure of FHL124 cells to 30  $\mu$ M H<sub>2</sub>O<sub>2</sub> for a 24-hour period resulted in a significant decrease in cell viability and a significant increase in cytotoxicity and

apoptosis (Fig. 2). In agreement with the above experiments, addition of 1  $\mu$ M SFN to the cells had no discernible effect on cell viability, cytotoxicity, or apoptosis relative to serum-free maintained control cells (Fig. 4). However, pretreatment of cells with 1  $\mu$ M SFN significantly inhibited H<sub>2</sub>O<sub>2</sub>-induced effects, such that cell viability, cytotoxicity, and apoptosis did not significantly differ from serum-free or SFN (alone) maintained cells (Fig. 4).

To support the ApoTox-Glo Triplex Assay (Promega) data, the LDH assay was used to assess cell damage/death. Treatment with 30  $\mu$ M hydrogen peroxide invoked a significant increase in LDH release into the medium (Fig. 5). This effect was inhibited by pretreatment of the cells with 1  $\mu$ M SFN. No difference in LDH levels was observed in the SFN-alone group compared with serum-free controls (Fig. 5).

Numerous prior studies have identified that oxidative stress induces DNA strand breaks in human cells.<sup>32,33</sup> To investigate such effects in this experimental system, the alkaline comet assay was used to investigate DNA strand breaks (and their repair) induced by oxidative stress in FHL124 cells over time. Exposure to 30  $\mu$ M H<sub>2</sub>O<sub>2</sub> resulted in the greatest levels of DNA strand breaks in cells harvested at the 30-minute time point, which demonstrated a mean value for DNA in the tail of 52.7% (Fig. 6). This declined with time, but remained significantly elevated at the 2-hour time point. There were significantly lower levels of DNA strand breaks if cells were pretreated with 1  $\mu$ M SFN (Fig. 6), indicating an enhanced antioxidant defense. Treatment with 1  $\mu$ M SFN alone for this time period did not significantly change levels of DNA strand breaks when compared with untreated cells.

To further test the protective nature of SFN against oxidative stress, we used a porcine whole-lens culture

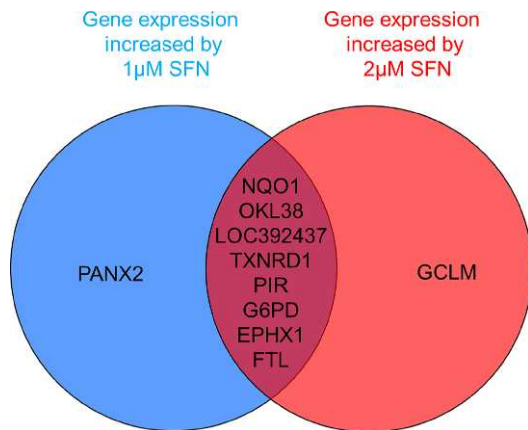


**FIGURE 8.** A Venn diagram showing the effect of 24-hour exposure of 1- and 2- $\mu$ M SFN on increased gene expression of FHL124 cells identified by Illumina gene microarray.

system.<sup>34</sup> Following dissection, whole porcine lenses did not demonstrate any notable opacity. Lenses maintained in serum-free medium remained transparent over the 4-day culture period. This is shown in Figure 7A, as the grid placed beneath the lens can be clearly seen. Similarly, with the dark-field image presented in Figure 7, minimal white light scattering regions are observed. Addition of 2  $\mu$ M SFN to the cultures did not affect transparency, such that lenses appeared similar to the serum-free control group. Exposure to 2 mM H<sub>2</sub>O<sub>2</sub> induced a marked change in transparency that appeared as a cloudiness in the peripheral cortex that progressed over time, such that most of the cortical region was affected (Fig. 7A). At day 1, the peripheral lens had begun to opacify, such that the grid could not be seen clearly through these regions (Fig. 7A) and was associated with light scatter (Fig. 7A). When 2 mM H<sub>2</sub>O<sub>2</sub> was added in the presence of 2  $\mu$ M SFN, opacity was still observed but this was less marked than the H<sub>2</sub>O<sub>2</sub>-only treated group. At end point (day 4), the culture medium was analyzed for LDH (Fig. 7B). Serum-free and SFN-only treated lenses had no discernible levels of LDH in the culture medium. Addition of hydrogen peroxide induced a dramatic increase in LDH levels, which was reduced in the presence of SFN.

### Identification of SFN Protective Mechanisms

As an initial screen to identify gene changes induced by SFN, an Illumina gene microarray was performed. The data revealed that nine genes were significantly upregulated following a 24-hour exposure to 1  $\mu$ M SFN (Table 1) and nine genes were also upregulated by 2  $\mu$ M SFN (Table 2). There were eight genes upregulated in both 1- and 2- $\mu$ M SFN exposures respectively (Fig. 8) (Table 1). NQO1 and TXNRD1 are classic phase II enzymes and were thus assessed using Western blot and immunocytochemistry to detect the protein products. In accordance with the microarray data, levels of NQO1 and TXNRD1 were significantly elevated in response to SFN. A concentration-dependent increase in NQO1 and TXNRD1 protein level was observed using Western blot methods (Fig. 9). Significant elevation was observed at SFN concentrations greater than or equal to 0.5  $\mu$ M, with a peak observed with 2  $\mu$ M SFN. This was a 2.5-fold elevation relative to untreated control cells for TXNRD1 (Fig. 9B). Similarly, NQO1 protein levels were increased by 2.3-fold compared with untreated control cells after 24-hour incubation with 2  $\mu$ M SFN (Fig. 9B). Protein expression was further evaluated using immunocytochemistry (Fig. 10). Using this approach, the distribution of both NQO1 and TXNRD1 was largely cytoplasmic. Quantifica-

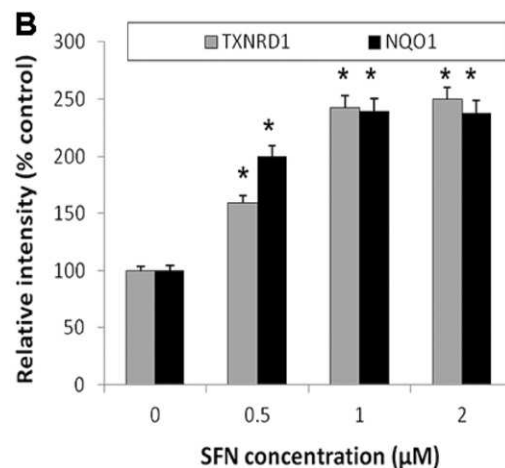
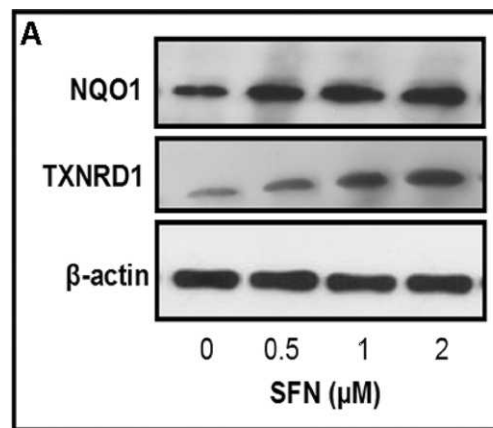


**FIGURE 9.** SFN induced NQO1 and TXNRD1 protein increase in FHL124 cells, detected using Western blot. (A) Representative blots showing NQO1, TXNRD1, and  $\beta$ -actin levels within FHL124 cells. (B) Quantitative data derived from band intensities; the protein band intensities for NQO1 and TXNRD1 were normalized to  $\beta$ -actin. Data are presented as mean  $\pm$  SEM ( $n = 4$ ). The asterisk indicates a significant difference between the treated and the nontreated control group ( $P \leq 0.05$ ; ANOVA with Dunnett's post hoc test).

tion of these images also demonstrated a significant increase in protein levels, such that with 2  $\mu$ M SFN, an 8-fold and 13-fold increase relative to untreated control cells was observed for NQO1 and TXNRD1, respectively (Fig. 10B).

### SFN Induction of Nrf2 Signaling in FHL124 Cells

As Nrf2 is a likely candidate in the regulation of SFN protection, further investigation was carried out to determine whether SFN could induce Nrf2 nuclear translocation in human lens epithelial cells. The accumulation and translocation of Nrf2 to the nucleus would indicate activation of Nrf2 and the induction of the Keap1-Nrf2-ARE pathway. Immunocytochemistry experiments were carried out to identify the location of Nrf2 proteins within FHL124 cells following SFN treatment for 4 hours. As shown in Figure 11A, only cytoplasmic labeling of Nrf2 with no distinct nuclear staining was observed in the nonstimulated cells, whereas an intense nuclear labeling was observed in the SFN-stimulated cells. In addition, the SFN treatment of the cells led to a dose-dependent increase in nuclear Nrf2 levels (Fig. 11B). These data clearly show that Nrf2 is translocated to the nucleus, indicating Keap1-Nrf2-ARE pathway activation in response to SFN exposure.

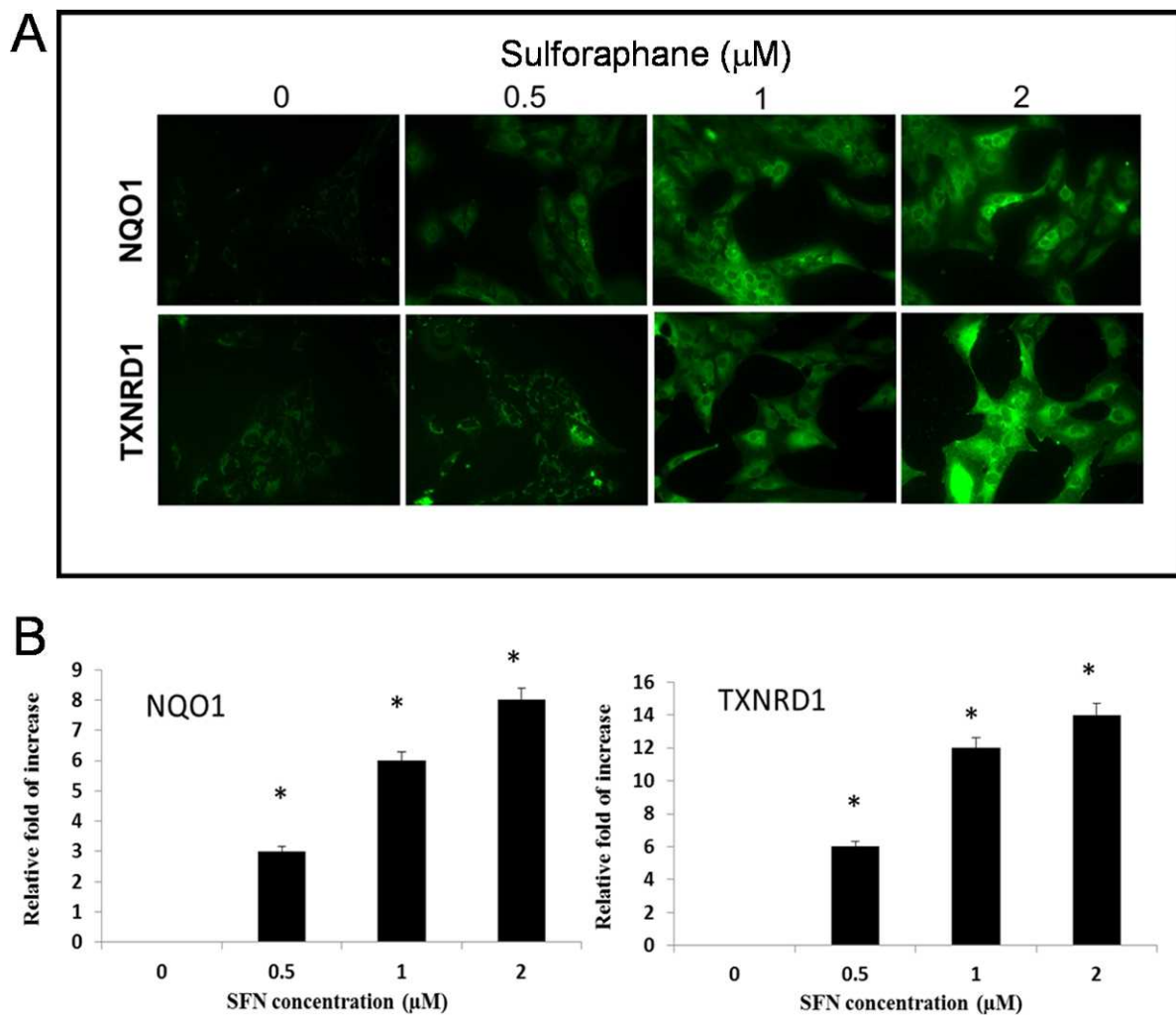


**FIGURE 10.** Immunocytochemical analyses of NQO1 and TXNRD1 distribution and expression within FHL124 cells following exposure to SFN for a 24-hour period. **(A)** Representative images showing the organization of NQO1 and TXNRD1 within FHL124 cells. **(B)** Quantitative data derived from fluorescence micrographs showing changes in protein level in response to SFN. Data are presented as mean  $\pm$  SEM ( $n = 4$ ). The *asterisk* indicates a significant difference between treated and control groups ( $P \leq 0.05$ ; ANOVA with Dunnett's post hoc test).

## DISCUSSION

Cataract is the major cause of blindness worldwide and cataract surgery is the most common surgical procedure performed on the elderly.<sup>3</sup> The large cost of this operation and possible complications associated with it favor long-term goals of avoiding cataract formation, or significantly retarding onset of the disease.

Epidemiological evidence suggests that high fruit and vegetable intake is associated with lower risk of any form of cataracts, although the mechanisms of protection are not known.<sup>35</sup> SFN has been identified in numerous cell and animal carcinogenesis models to be an effective chemopreventive agent, which uses a diverse range of molecular mechanisms to achieve this.<sup>20</sup> The current work demonstrates that pretreatment with SFN, which is abundant in green vegetables, such as broccoli, yielded protection for lens epithelial cells against hydrogen peroxide-induced DNA damage, cell death, and transparency loss. It is therefore of interest to consider the mechanisms by which SFN provides this protection.<sup>19</sup> Putative mechanisms include a direct interaction with the oxidative stressor ( $\text{H}_2\text{O}_2$ ), inhibition of apoptotic signals, or via

modification of DNA repair systems enhancing activity of antioxidant defense enzymes.<sup>36</sup>

From the experimental data, it is unlikely that SFN causes its effect by direct antioxidant actions because with cotreatment no significant protection was observed; to achieve protection, pretreatment was required. ITCs can rapidly accumulate in human and animal cells, with the peak intracellular ITC accumulation reached within 0.5 to 3.0 hours of exposure and up to 100- to 200-fold over the extracellular ITC concentration.<sup>37,38</sup> This suggests modification to the cell occurs to enhance protection or that transport of SFN to key areas within the cells takes time. It is clear SFN can be readily accumulated in cells, but it is unclear how modification of SFN itself could influence the beneficial outcomes observed. SFN reacts with glutathione to give rise to a glutathione-SFN conjugate, which is catalyzed by Glutathione-S-Transferases.<sup>38</sup> After that, stepwise cleavage of glutamine and glycine first by the enzymes  $\gamma$ -glutamyl transpeptidase and then by cysteinylglycinase yields an L-cysteine conjugate. Then N-acetyltransferase acetylates the L-cysteine conjugate to produce N-acetyl-L-cysteine conjugate (mercapturic acid derivative). Understanding the molecular life cycle of SFN and its derivatives in lens cells over time will be of great interest and may provide further understanding

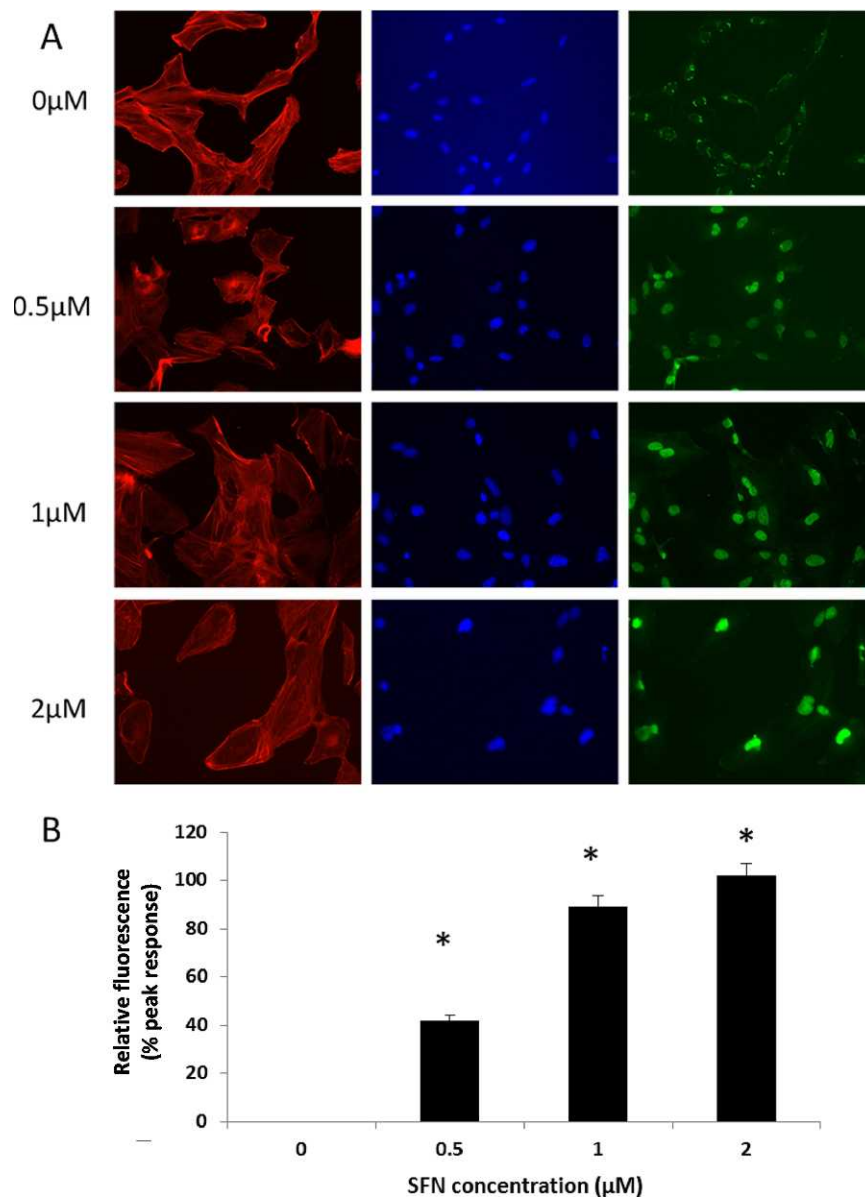


**FIGURE 11.** SFN induction of nuclear translocation of Nrf2 in FHL124 cells. **(A)** Representative fluorescent micrographs showing Nrf2 (green) distribution following a 4-hour exposure to 0-, 0.5-, 1-, and 2-μM SFN treatment. Nuclei and actin filaments are labeled using DAPI (blue) and Texas red X-Phalloidin (red), respectively. **(B)** Quantitative data derived from fluorescence micrographs showing changes in nuclear protein level in response to SFN. Data are presented as mean  $\pm$  SEM ( $n = 4$ ). The asterisk indicates a significant difference between treated and control groups ( $P \leq 0.05$ ; ANOVA with Dunnett's post hoc test).

of how SFN can be regulated to provide maximum benefit to an individual. Establishing a greater understanding of when pretreatment of SFN is effective and the point at which peak levels are observed in both cultured cells and within the lens will be of great interest for future studies.

DNA strand breaks detected using the alkaline comet assay were reduced by SFN pretreatment. This may be a result of upstream effects of SFN giving rise to less damage or because of the increased efficiency of mechanisms that repair DNA strand breaks, such as nonhomologous end joining.<sup>36</sup> This can be tested in the future by the use of small interfering RNA (siRNA) knockdowns of the repair systems. If upstream factors reduce DNA damage, then no difference will be observed by reduction of DNA repair capacity.

Modification of enzymatic antioxidant defense systems is also likely to play a key role and the data presented support

this notion. Dietary ITCs are breakdown products of glucosinolates from cruciferous vegetables, for example, broccoli.<sup>20</sup> There are many studies that demonstrate ITCs are potent inducers of chemopreventive enzymes, including antioxidant enzymes.<sup>39,40</sup> The current study has addressed this issue by an Illumina gene array to determine the effects of SFN on gene expression. The data revealed that eight genes were significantly upregulated following 24-hour exposure to both 1- and 2-μM SFN, of which a number are associated with antioxidant defense. Of the genes that were upregulated, all are reported in the literature to be controlled by the transcription factor Nrf2. TXNRD1 and NQO1 are classic phase II enzymes and have been reported to show increased expression in a number of cells and tissues.<sup>41</sup> G6PD encodes glucose-6-phosphate dehydrogenase, which is a cytosolic enzyme whose primary function is to produce NADPH; this gene is also reported to

be regulated by Nrf2 signaling.<sup>42</sup> Moreover, NADPH is used by NQO1 as a hydride donor in the conversion of quinones to hydroquinones. Therefore, upregulation of G6PD is likely to facilitate the antioxidant activity of NQO1. Nrf2 signaling has also been implicated in the expression of pirin in small airway epithelium. In smokers, Nrf2 signaling was more active and this was associated with increased expression of pirin relative to nonsmokers.<sup>43</sup> Moreover, it was identified that the promoter region of the pirin gene contains functional antioxidant response elements.<sup>43</sup> In addition, EPHX1 and FTL, which encode epoxide hydrolase 1 and ferritin light chain, respectively, were also shown in a mouse model to be induced by 1-(2-cyano-3-,12-dioxooleana-1,9[11]-dien-28-oyl)imidazole (CDDO-Im), which is a highly potent chemopreventive agent. In Nrf2 knockout animals, the induction of EPHX1 was suppressed indicating an important role of Nrf2 signaling in its regulation.<sup>44</sup> In the case of FTL, the CDDO-Im induced expression was ablated in the absence of Nrf2.<sup>45</sup> OKL38, which encodes oxidative stress-induced growth inhibitor 1, is reported to show induction following oxidative stress.<sup>46</sup> In cancer cells, it is believed that following DNA strand breaks, OKL38 interacts with p53 and relocates to the mitochondrion to initiate cytochrome c release and apoptosis; OKL38 is therefore defined as a tumor suppressor.<sup>47</sup> In the current system, OKL38 is upregulated in response to SFN, but under these conditions, cells continue to survive and grow. In addition, cytotoxicity/apoptosis does not differ from controls. Oxidative stress-induced DNA damage is suppressed by SFN and perhaps without this cue, OKL38 does not interact with p53 and induce apoptosis. The expression of OKL38 remains curious and further inhibition studies will be required to elucidate its putative role in SFN protection in the lens.

The common factor linking all the genes shown to be upregulated is Nrf2/keap1 signaling. It was therefore of importance to establish whether Nrf2 signaling can take place in lens cells in response to SFN. The data confirm that Nrf2 translocation does occur and thus it is reasonable to hypothesize that the protection observed with SFN against oxidative stress is largely mediated by Nrf2 regulation. SFN is known to influence this pathway through interaction with the thiol group on keap1, which liberates Nrf2 from the complex. Nrf2 then translocates to the nucleus and initiates transcription.<sup>20</sup> It will therefore be of great interest in the future to determine more of the role of Nrf2 in expression of the genes identified from the microarray data. Such work will involve establishing the kinetics of Nrf2 nuclear translocation in response to SFN using immunocytochemistry and GFP tags, Nrf2/ARE reporter assays, and siRNA approaches to assess functional involvement of the individual genes and Nrf2 signaling.

In summary, pretreatment of cells or whole lenses with SFN can modify antioxidant defense mechanisms by induction of the Keap1-Nrf2-ARE pathway, thus rendering lens cells more capable of suppressing the daily insult of oxidative stress. Improved intake through an SFN-rich diet or use of supplements could provide a novel approach to retard the onset of cataract formation in the human lens.

### Acknowledgments

The authors thank Sarah Russell for cell culture assistance and Julie Eldred for technical advice.

Supported by The Humane Research Trust.

Disclosure: **H. Liu**, None; **A.J.O. Smith**, None; **M.C. Lott**, None; **Y. Bao**, None; **R.P. Bowater**, None; **J.R. Reddan**, None; **I.M. Wormstone**, None

### References

- Javitt JC, Wang F, West SK. Blindness due to cataract: epidemiology and prevention. *Annu Rev Public Health*. 1996;17:159-177.
- Taylor A. Cataract: relationship between nutrition and oxidation. *J Am Coll Nutr*. 1993;12:138-146.
- Wormstone IM, Wang L, Liu CS. Posterior capsule opacification. *Exp Eye Res*. 2009;88:257-269.
- Spector A. Oxidative stress-induced cataract: mechanism of action. *FASEB J*. 1995;9:1173-1182.
- Droge W. Free radicals in the physiological control of cell function. *Physiol Rev*. 2002;82:47-95.
- Evans P, Halliwell B. Free radicals and hearing. Cause, consequence, and criteria. *Ann N Y Acad Sci*. 1999;884:19-40.
- Finkel T, Holbrook NJ. Oxidants, oxidative stress and the biology of ageing. *Nature*. 2000;408:239-247.
- Lou MF. Redox regulation in the lens. *Prog Retin Eye Res*. 2003;22:657-682.
- Brennan LA, Kantorow M. Mitochondrial function and redox control in the aging eye: role of MsrA and other repair systems in cataract and macular degenerations. *Exp Eye Res*. 2009;88:195-203.
- Holmgren A. Thioredoxin and glutaredoxin systems. *J Biol Chem*. 1989;264:13963-13966.
- Chrestensen CA, Eckman CB, Starke DW, Mיעyal JJ. Cloning, expression and characterization of human thioltransferase (glutaredoxin) in *E. coli*. *FEBS Lett*. 1995;374:25-28.
- Raghavachari N, Lou MF. Evidence for the presence of thioltransferase in the lens. *Exp Eye Res*. 1996;63:433-441.
- Hansson HA, Holmgren A, Norstedt G, Rozell B. Changes in the distribution of insulin-like growth factor I, thioredoxin, thioredoxin reductase and ribonucleotide reductase during the development of the retina. *Exp Eye Res*. 1989;48:411-420.
- Bhuyan KC, Reddy PG, Bhuyan DK. Thioredoxin genes in lens: regulation by oxidative stress. *Methods Enzymol*. 2002;347:421-435.
- Raghavachari N, Krysan K, Xing K, Lou MF. Regulation of thioltransferase expression in human lens epithelial cells. *Invest Ophthalmol Vis Sci*. 2001;42:1002-1008.
- Reddy PG, Bhuyan DK, Bhuyan KC. Lens-specific regulation of the thioredoxin-1 gene, but not thioredoxin-2, upon in vivo photochemical oxidative stress in the emery mouse. *Biochem Biophys Res Commun*. 1999;265:345-349.
- Beswick HT, Harding JJ. Conformational changes induced in bovine lens alpha-crystallin by carbamylation. Relevance to cataract. *Biochem J*. 1984;223:221-227.
- Lou MF, Dickerson JE Jr. Protein-thiol mixed disulfides in human lens. *Exp Eye Res*. 1992;55:889-896.
- Cheung KL, Kong AN. Molecular targets of dietary phenethyl isothiocyanate and sulforaphane for cancer chemoprevention. *AAPS J*. 2010;12:87-97.
- Juge N, Mithen RF, Traka M. Molecular basis for chemoprevention by sulforaphane: a comprehensive review. *Cell Mol Life Sci*. 2007;64:1105-1127.
- Hintze KJ, Keck AS, Finley JW, Jeffery EH. Induction of hepatic thioredoxin reductase activity by sulforaphane, both in Hepa1c1c7 cells and in male Fisher 344 rats. *J Nutr Biochem*. 2003;14:173-179.
- Tanito M, Masutani H, Kim YC, Nishikawa M, Ohira A, Yodoi J. Sulforaphane induces thioredoxin through the antioxidant-responsive element and attenuates retinal light damage in mice. *Invest Ophthalmol Vis Sci*. 2005;46:979-987.
- Wagner AE, Ernst I, Iori R, Desel C, Rimbach G. Sulforaphane but not ascorbigen, indole-3-carbinol and ascorbic acid activates the transcription factor Nrf2 and induces phase-2

- and antioxidant enzymes in human keratinocytes in culture. *Exp Dermatol*. 2010;19:137-144.
24. Ye L, Dinkova-Kostova AT, Wade KL, Zhang Y, Shapiro TA, Talalay P. Quantitative determination of dithiocarbamates in human plasma, serum, erythrocytes and urine: pharmacokinetics of broccoli sprout isothiocyanates in humans. *Clin Chim Acta*. 2002;316:43-53.
  25. Reddan JR, Giblin FJ, Kadry R, Leverenz VR, Pena JT, Dziedzic DC. Protection from oxidative insult in glutathione depleted lens epithelial cells. *Exp Eye Res*. 1999;68:117-127.
  26. Wormstone IM, Tamiya S, Eldred JA, et al. Characterisation of TGF-beta2 signalling and function in a human lens cell line. *Exp Eye Res*. 2004;78:705-714.
  27. Lim SY, Chung WY, Lee HK, Park MS, Park HG. Direct and nondestructive verification of PNA immobilization using click chemistry. *Biochem Bioph Res Co*. 2008;376:633-636.
  28. Smyth GK. Linear models and empirical bayes methods for assessing differential expression in microarray experiments. *Stat Appl Genet Mol Biol*. 2004;3:Article3.
  29. McCarthy DJ, Smyth GK. Testing significance relative to a fold-change threshold is a TREAT. *Bioinformatics*. 2009;25:765-771.
  30. Benjamini Y, Yekutieli D. Quantitative trait Loci analysis using the false discovery rate. *Genetics*. 2005;171:783-790.
  31. Schneider CA, Rasband WS, Eliceiri KWNH. Image to ImageJ: 25 years of image analysis. *Nat Methods*. 2012;9:671-675.
  32. Liu J, Wang Y, Cui J, et al. Ochratoxin A induces oxidative DNA damage and G1 phase arrest in human peripheral blood mononuclear cells in vitro. *Toxicol Lett*. 2012;211:164-171.
  33. Jantzen K, Roursgaard M, Desler C, Loft S, Rasmussen LJ, Moller P. Oxidative damage to DNA by diesel exhaust particle exposure in co-cultures of human lung epithelial cells and macrophages. *Mutagenesis*. 2012;27:693-701.
  34. Tamiya S, Wormstone IM, Marcantonio JM, Gavrilovic J, Duncan G. Induction of matrix metalloproteinases 2 and 9 following stress to the lens. *Exp Eye Res*. 2000;71:591-597.
  35. Cumming RG, Mitchell P, Smith W. Diet and cataract: the Blue Mountains Eye Study. *Ophthalmology*. 2000;107:450-456.
  36. Polo SE, Jackson SP. Dynamics of DNA damage response proteins at DNA breaks: a focus on protein modifications. *Genes Dev*. 2011;25:409-433.
  37. Zhang Y. Molecular mechanism of rapid cellular accumulation of anticarcinogenic isothiocyanates. *Carcinogenesis*. 2001;22:425-431.
  38. Zhang Y. The molecular basis that unifies the metabolism, cellular uptake and chemopreventive activities of dietary isothiocyanates. *Carcinogenesis*. 2012;33:2-9.
  39. Keum YS, Jeong WS, Kong AN. Chemopreventive functions of isothiocyanates. *Drug News Perspect*. 2005;18:445-451.
  40. Thornalley PJ. Isothiocyanates: mechanism of cancer chemopreventive action. *Anticancer Drugs*. 2002;13:331-338.
  41. Matusheski NV, Jeffery EH. Comparison of the bioactivity of two glucoraphanin hydrolysis products found in broccoli, sulforaphane and sulforaphane nitrile. *J Agric Food Chem*. 2001;49:5743-5749.
  42. Shelton P, Jaiswal AK. The transcription factor NF-E2-related factor 2 (Nrf2): a protooncogene? *FASEB J*. 2013;27:414-423.
  43. Hubner RH, Schwartz JD, De Bishnu P, et al. Coordinate control of expression of Nrf2-modulated genes in the human small airway epithelium is highly responsive to cigarette smoking. *Molecular medicine*. 2009;15:203-219.
  44. Malhotra D, Portales-Casamar E, Singh A, et al. Global mapping of binding sites for Nrf2 identifies novel targets in cell survival response through ChIP-Seq profiling and network analysis. *Nucleic Acids Res*. 2010;38:5718-5734.
  45. Liby K, Hock T, Yore MM, et al. The synthetic triterpenoids, CDDO and CDDO-imidazolide, are potent inducers of heme oxygenase-1 and Nrf2/ARE signaling. *Cancer Res*. 2005;65:4789-4798.
  46. Li R, Chen W, Yanes R, Lee S, Berliner JA. OKL38 is an oxidative stress response gene stimulated by oxidized phospholipids. *J Lipid Res*. 2007;48:709-715.
  47. Hu J, Yao H, Gan F, Tokarski A, Wang Y. Interaction of OKL38 and p53 in regulating mitochondrial structure and function. *PLoS One*. 2012;7:e43362.